

## ANALYSIS OF THE HEAT CAPACITIES OF GROUP IV CHALCOGENIDES USING DEBYE TEMPERATURES

U. GAUR, G. PULTZ, H. WIEDEMEIER and B. WUNDERLICH

*Department of Chemistry, Rensselaer Polytechnic Institute, Troy, New York 12181, U.S.A.*

(Received December 18, 1980)

The low temperature heat capacities of 13 group IV chalcogenides are examined. The heat capacity of crystals with largely isotropic structure (GeTe, SnSe, SnTe, PbS, PbSe, PbTe) can be represented within  $\pm 3\%$  by a three-dimensional Debye function ( $\theta_3 = 205, 230, 175, 225, 150$  and  $130$ , respectively). The heat capacity of crystals with anisotropic structures (GeS, GeSe, SnS, GeS<sub>2</sub> and SnS<sub>2</sub>) could only be represented by pairs of two-dimensional Debye functions for the longitudinal and transverse lattice vibrations (error  $\pm 0.5$  to  $3\%$ ;  $\theta_2(l) = 505, 345, 400, 705, 480$  and  $570$ , respectively, and  $\theta_2(t) = 200, 185, 160, 175, 100$  and  $265$ , respectively).

Since the two-dimensional Debye function has not been tabulated in detail, we offer in the appendix a five place table of it. Raman and infrared data support this analysis.

Low temperature heat capacities are often well described by the Debye approach [1]. In extensive reviews [2, 3] it was shown earlier that a single  $\theta$ -temperature could represent the heat capacity at constant volume for many elements and simple compounds adequately up to about  $30$ . For two-dimensional and one-dimensional crystals, analogous two-dimensional and one-dimensional Debye functions can be derived [4–6]. The one-dimensional Debye function alone and in combination with a three-dimensional Debye function (Tarasov function) found widespread application in the description of heat capacities of linear macromolecules [7]. Two-dimensional Debye functions were used to describe heat capacities for crystals with layer structures such as graphite and boron nitride [4, 6, 8]. Tables of the Debye functions, which are somewhat cumbersome to calculate, are widely available for the three-dimensional case [9]. A one-dimensional Debye function table was published by us earlier [10]. Since there seems to be no tabulation [11] of a precision two-dimensional Debye function table, we included such a table in the appendix.

The class IV chalcogenide crystals fall into two groups. One has a largely isotropic crystal structure, the other a layer-type structure. It will be shown that the model for heat capacity description must take, as expected, this fact into account.

Our initial interest in group IV chalcogenides arose from the study of vapor transport properties [12, 13]. For the interpretation of these, accurate values of enthalpies, entropies and Gibbs free energies are needed. Since heat capacities are usually not available to the lowest temperatures, we undertook the present study which includes 13 different group IV chalcogenides (see Table 1).

Table 1  
Group IV chalcogenides and their low temperature  
heat capacity expressions

Compound	Crystal structure	$C_p$ references	$A_0^a$ for $\theta_s$ (Kmol/J) $\times 10^3$	$\theta_s$	% Error in $C_v$ from $\theta_s$	$\theta_s(t)$	$\theta_s(t)$	% Error in $C_v$ from $\theta_s$
GeS	orthorhombic (double-layers)	16, 17, 22	—	—	—	200	505	< $\pm 2.0^d$
GeGe	orthorhombic (double-layers)	16, 17, 22	5.12	270	< $\pm 2.0^b$	185	345	< $\pm 0.5$
GeTe	rhombohedral	17, 18, 20	10.24	205	< $\pm 1.0^b$	—	—	—
SnS	orthorhombic (double-layers)	23	5.12	300	< $\pm 2.0^b$	160	400	< $\pm 3.0^d$
SnSe	orthorhombic (double-layers)	21	10.24	230	— <sup>c</sup>	—	—	—
SnTe	cubic	20	5.12	175	— <sup>c</sup>	—	—	—
PbS	cubic	19	5.12	225	< + 0.5 <sup>b</sup>	—	—	—
PbSe	cubic	19	5.12	150	< $\pm 3.0^b$	—	—	—
PbTe	cubic	19	5.12	130	< $\pm 2.0^b$	—	—	—
GeSe <sub>2</sub>	orthorhombic (double-layers)	24	—	—	< $\pm 3.0^d$	175	705	< $\pm 3.0^d$
GeSe <sub>2</sub>	orthorhombic (double-layers)	24	—	—	—	100	480	< $\pm 1.0^d$
SnS <sub>2</sub>	hexagonal (triple-layers)	23	—	—	—	—	265	< $\pm 1.5^d$
SnSe	hexagonal (triple-layers)	21	—	—	—	—	—	—

<sup>a</sup> per mole of atoms

<sup>b</sup> from 100K to 250K

<sup>c</sup> insufficient data to determine  $\theta$  accurately

<sup>d</sup> for 50K to 250 K

<sup>e</sup> no data available below 220 K

### Application of the three-dimensional Debye function

The analysis of heat capacities of group IV–VI compounds below 200 K is based on five approximation methods: The addition of contributions of the constituent elements [14, 15], the use of the Debye model [16–21], the application of a combined Debye and Einstein model [14, 22, 23], the fit to the Tarasov model [16], and the approximation to an exponential function ( $C_p = AT^n$ ) [16, 18, 24]. Most of these analyses had little or no structural justification.

We began our analysis with the application of the three-dimensional Debye model

$$C_v = 9 Nk \left[ \frac{T}{\theta_3} \right]^3 \int_0^{\theta_3} \frac{x^3 dx}{e^x - 1} - \frac{\theta_3/T}{e^{(\theta_3/T)} - 1} \quad (1)$$

or abbreviated, for one mole of vibrators

$$C_v = 3RD_3(\theta_3/T) \quad (2)$$

The expression  $D(\theta_3/T)$  is the three-dimensional Debye function,  $\theta_3$  is the three-dimensional Debye temperature, and  $x$  represents  $h\nu/kT$ . The relationship between the measured  $C_p$  and  $C_v$  is

$$C_p - C_v = \alpha^2 VT/k \quad (3)$$

where  $\alpha$  is the isothermal expansivity,  $K$  is the isothermal compressibility and  $V$  is the molar volume of the solid. Since  $\alpha$  and  $K$  are not commonly measured, and are not available for the group IV chalcogenides, we assume as a first approxima-

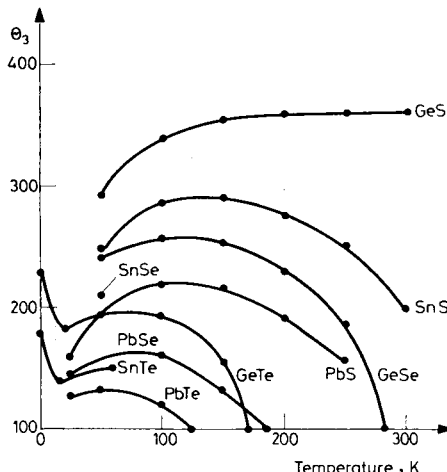


Fig. 1.  $\theta_3$  as a function of temperature for group IV monochalcogenides.  $\theta_3$  was calculated from  $C_p$

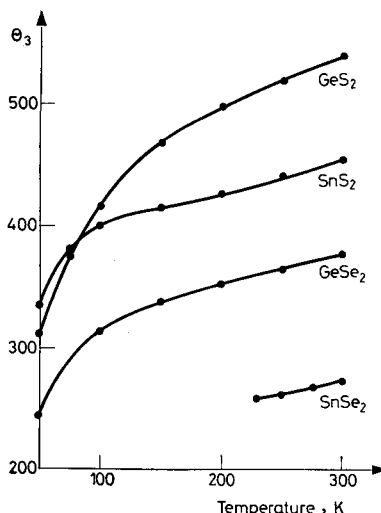


Fig. 2.  $\theta_3$  as a function of temperature for group IV dichalcogenides.  $\theta_3$  was calculated from  $C_p$

tion, that up to 300 K  $C_p$  is essentially equal to  $C_v$ . A plot of calculated  $\theta_3$  values from the experimental  $C_p$  values for the various group IV chalcogenides is shown in Figs 1 and 2. All group IV chalcogenides show considerable variation in  $\theta_3$  with temperature, as indication of serious shortcomings of the approach. The decrease in  $\theta_3$  with increasing temperature occurs when  $C_p$  approaches the upper limit for  $C_v$  of  $6R$  for binary compounds or of  $9R$  for ternary compounds. In this temperature range the  $\theta_3$  calculation is particularly sensitive to the difference between  $C_p$  and  $C_v$ . As a second approximation we employed several methods to estimate the  $C_p - C_v$  difference and corrected the  $\theta_3$  calculation. A commonly used approximation was introduced by Nernst and Lindemann [25]. For elements and ionic solids they suggest

$$C_p - C_v = A_0 \cdot C_p^2 T / T_m, \quad (4)$$

where  $T_m$  is the melting temperature and  $A_0$  is a constant determined to be  $5.12 \times 10^{-3}$  K mol/J. (Note that this constant is defined per mole of atoms.) Nernst and Lindemann show in their listed values of  $A_0$  a variation from  $2.4 \times 10^{-3}$  to  $9.6 \times 10^{-3}$  K mol/J [25]. Changing the experimental  $C_p$  values with the help of Eq. 4 into  $C_v$  leads to the  $\theta_3$  values plotted in Figs 3 and 4. Some of the mono-chalcogenides show now a largely constant  $\theta_3$  value with only minor fluctuations (particularly the lead chalcogenides, GeSe and SnS), while GeS and the dichalcogenides (Fig. 4) still show extensive variation of  $\theta_3$  with temperature.

As mentioned above, the error in  $A_0$  is about  $\pm 50\%$ . Allowing  $A_0$  to go to its upper limit,  $C_p - C_v$  was recalculated and  $\theta_3$  values obtained. These are shown in Figs 5 and 6. In this case,  $\theta_3$  is practically temperature independent for the

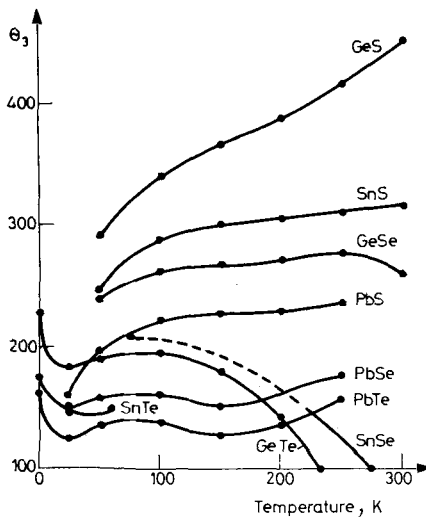


Fig. 3.  $\theta_3$  as a function of temperature for group IV monochalcogenides.  $\theta_3$  was calculated from  $C_v$  using the Nernst–Lindemann approximation with  $A_0 = 5.12 \times 10^{-6}$  K mol/J

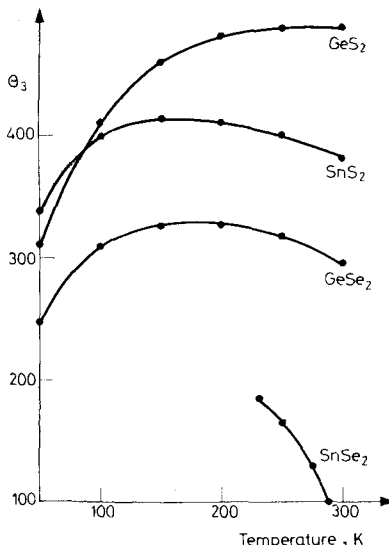


Fig. 4.  $\theta_3$  as a function of temperature for group IV dichalcogenides.  $\theta_3$  was calculated from  $C_v$  determined by the Nernst–Lindemann approximation with  $A_0 = 5.12 \times 10^{-6}$  K mol/J

additional compounds GeTe and SnSe. The previously shown temperature independence of  $\theta_3$  for GeSe and SnS (Fig. 3) now reveals a considerable increase of  $\theta_3$  with temperature. The corresponding behaviour of the dichalcogenides is even

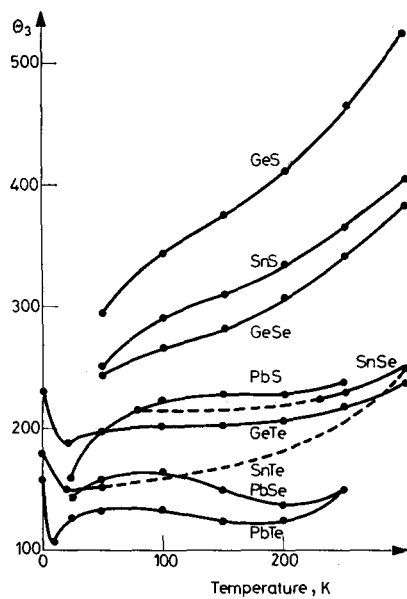


Fig. 5.  $\Theta_3$  as a function of temperature for group IV monochalcogenides.  $\Theta_3$  was calculated from  $C_v$  determined by the Nernst—Lindemann approximation with  $A_0 = 1.02 \times 10^{-2} \text{ K mol/J}$

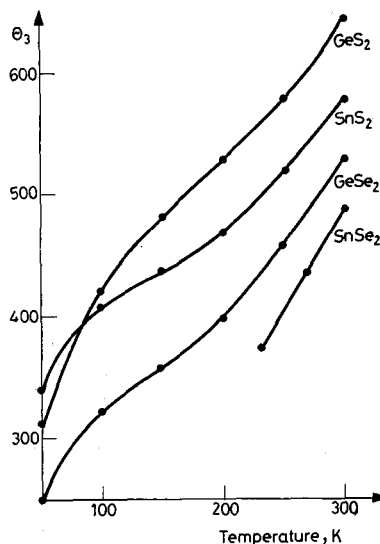


Fig. 6.  $\Theta_3$  as a function of temperature for group IV dichalcogenides.  $\Theta_3$  was calculated from  $C_v$  determined by the Nernst—Lindemann approximation with  $A_0 = 1.02 \times 10^{-2} \text{ K mol/J}$

more pronounced (Fig. 6). To test the validity of the Nernst-Lindemann approximation, we looked for experimental data to use in Eq. 3. Data were only available for GaSe [26], which exhibits a layer-type crystal structure similar to some group IV compounds. The  $C_p - C_v$  difference was found to be about one half the value predicted by the Nernst-Lindemann equation. (Note that values calculated by Aliev *et al.* [26] for GaSe using the Nernst-Lindemann expression are too large by a factor of two since they use  $A_0$  "per atom" and  $C_p$  "per molecule".) Still, the values for  $C_p - C_v$  are within the rather wide error margin of the constant  $A_0$ .

While the difference between  $C_p$  and  $C_v$  can be used to explain the curvature in some of the  $\theta_3$  vs.  $T$  curves at high temperature, no reasonable change in  $A_0$  can be found to eliminate the steep drop in  $\theta_3$  at low temperature for GeS and the dichalcogenides. Thus,  $\theta_3$  cannot be used as an extrapolation for their low temperature heat capacities. Table 1 lists the  $\theta_3$  values only for crystals whose heat capacities can be adjusted to yield an approximately constant  $\theta_3$  value with reasonable values for  $A_0$ .

### Two-dimensional Debye functions

The group IV chalcogenides vary in crystal structure from cubic, covalently bonded structures such as SnTe [27] to orthorhombic, layer-type structures of GeS<sub>2</sub> and GeSe<sub>2</sub> [28]. The compounds GeS, GeSe and SnS occupy an intermediate position, since they exhibit layer-type structures at low temperatures, but either transform to cubic symmetry (GeSe [29]) or approach a more isotropic structure (GeS [30], SnS [31, 32]) with increasing temperature. For the series of compounds, GeS, GeSe, SnS and SnSe, X-ray diffraction studies [32] have shown that the degree of anisotropic character decreases in the following order

$$\text{GeS} \approx \text{GeSe} > \text{SnS} \approx \text{SnSe} \gg \text{GeTe} > \text{SnTe}.$$

It is apparent that only  $C_p$  of the more isotropic compounds can be approximated by the three-dimensional Debye function.

A comparison can now be made between the layer-type structures of some group IV-VI compounds and graphite. The orthorhombic studies of some monochalcogenides (GeS, GeSe, SnS, SnSe) consist of sets of double-layers with strong primary bonding within the double-layers and weak, secondary bonding between adjacent sets of double layers [27, 29, 32]. A more detailed discussion of the structures of the above monochalcogenides is found elsewhere [32]. The dichalcogenides exhibit either an orthorhombic double-layer structure (GeS<sub>2</sub> and GeSe<sub>2</sub>) [28] or a hexagonal CdI<sub>2</sub>-type structure (SnS<sub>2</sub> and SnSe<sub>2</sub>) [32] composed of sets of triple-layers. With respect to the layer-type structure of graphite, the heat capacity of the layer-type IV-VI compounds could be expected to show a similar behaviour.

The heat capacity of graphite cannot be approximated by standard Debye theory, and as early as 1911 Nernst [35] suggested two "Einstein temperatures"

instead of a single characteristic temperature to be used. Tarasov [4] suggested a two-dimensional Debye function to describe the heat capacity behavior of graphite. This method was modified by several authors [6, 36], culminating in the extension of the Debye theory by Krumhansl and coworkers [8]. Simply stated, the lattice vibrations were divided into the transverse and longitudinal vibrations. Because of the strong anisotropy of graphite the transverse vibrations are expected to be of higher frequency. The overall expression for heat capacity is thus

$$C_v = R \left[ D_2 \left( \frac{\theta_2(t)}{T} \right) + 2D_2 \left( \frac{\theta_2(l)}{T} \right) \right], \quad (6)$$

where  $D_2(\theta_2/T)$  is the two-dimensional Debye function

$$D_2 \left( \frac{\theta_2}{T} \right) = 2 \left( \frac{T}{\theta_2} \right)^2 \int_0^{\theta_2/T} \frac{x^3 e^x}{(e^x - 1)^2} dx \quad (7)$$

Besides for graphite and boron nitride,  $D_2$  fits have been attempted to interpret heat capacities of some layered organocupper compounds [37]. Measured graphite heat capacities ( $C_p$ ) can be fitted to this combination  $D_2$  function from 0–1000 K, partially due to the small difference between  $C_p$  and  $C_v$  for graphite. In attempting to fit group IV chalcogenides to Eq. 7,  $C_v$  values calculated by the Nernst–Lindemann approximation were used. New tables were generated for  $\theta_2/T$  from 0.00 to 17.50 in increments of 0.01. These are shown in the appendix. The resulting values of  $\theta_2(l)$  and  $\theta_2(t)$  for the layer-type crystals of the group IV chalcogenides are shown in Table 1. All listed  $\theta_2$ -temperatures yielded  $C_v$  values in the temperature range 50–250 K within  $\pm 3\%$ . Note that while  $\theta_3$  is fairly constant with temperature for GeSe and SnS, the  $C_v$  data for these compounds

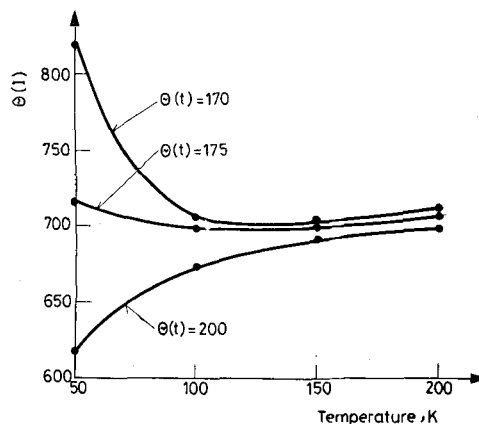


Fig. 7. The variation of  $\theta_2(t)$  with temperature for a given  $\theta_2(l)$  for  $\text{GeS}_2$

can still be fitted to the two-dimensional expression with good results. Other compounds (such as GeTe) cannot be fitted to the two-dimensional form with any degree of agreement. For these only  $\theta_3$  data were listed in Table 1. Figure 7 shows the effect of choosing different values of  $\theta_2(t)$  for  $\text{GeS}_2$ . It is apparent that within narrow limits the  $\theta_2$  temperatures are fixed.

### Discussion

Considering only the measured heat capacities of group IV-VI compounds, it was possible to decide on a three- or two-dimensional Debye function fit. In this discussion it is attempted to correlate the two-dimensional Debye constants with the actual crystal structure of these compounds.

Raman and infrared spectroscopy [38-43] have been used to determine the relative strength of intralayer and interlayer bonding in group IV monochalcogenides and other layered compounds. Using the ratio of intralayer to interlayer force constants as a measure of anisotropy of the crystal structure, the degree of anisotropy is estimated to decrease in the following order [38, 39, 41],

$$\text{GeSe} \gtrsim \text{GeS} > \text{SnS} \gtrsim \text{SnSe}. \quad (8)$$

The overall trend of decreasing anisotropy is in agreement with that based on the consideration of structural data (Eq. 5) [33]. The above trend (Eq. 8) is consistent with the data in Table 1, which show that  $\theta_2(l)$  for all two-dimensional fits is greater than  $\theta_2(t)$ . Since  $\theta_2$  is related to vibrations within the solid by the expression

$$\theta_2(l, t) = v(l, t)h/k, \quad (9)$$

the greater  $\theta_2(l)$  indicates a larger intralayer frequency (thus larger force constant) relative to the interlayer frequency ( $\theta_2(t)$ ).

$\text{SnS}_2$  and  $\text{SnSe}_2$  are even more layer-like, with estimates of the force constant ratio being of the order of 100 [42]. Spectroscopic data for  $\text{GeS}_2$  and  $\text{GeSe}_2$  are not available, but using their structure for an estimate, the force constant ratio of these compounds would probably be between that of  $\text{SnS}_2$  and of the monochalcogenides.

Thus, all heat capacities which could be fitted to a two-dimensional Debye function exhibit layer-type structures, and the relative values of  $\theta_2(l)$  and  $\theta_2(t)$  are in agreement with the expected values for layer-type structures. Unfortunately, a more quantitative comparison of observed spectroscopic vibrations to  $\theta_2(l)$  and  $\theta_2(t)$  is prohibited due to a lack of such data for  $\text{GeS}_2$  and  $\text{GeSe}_2$  and due to orientation dependencies of spectroscopic vibrations. However, the evidence presented suggests that the two-dimensional solutions are related to the vibrational modes of these IV-VI compounds.

The authors would like to acknowledge the help of Professor H. H. Hollinger and Professor M. S. Krishnamoorty with the solution of the two-dimensional Debye function. The authors would also like to acknowledge the support of this work in part by the National Aeronautics and Space Administration and by the National Science Foundation, Polymer Programs, Contract No. DMR 78-15279.

### References

1. P. DEBYE, Ann. Physik, 39 (1912) 789.
2. A. EUCKEN, Handbuch der Experimentalphysik, VIII (I), Ch. 5, 1929.
3. E. SCHRÖDINGER, Handbuch der Experimentalphysik, X 1926, p. 275.
4. V. V. TARASOV, Compt. Rend. Acad. Sci. URSS, 46 (1945) 110; ibid. 54 (1946) 795; Zh. Fiz. Khim., 24 (1950) 111; ibid. 27 (1953) 1430; Dokl. Akad. Nauk SSSR, 100 (1955) 307.
5. V. V. TARASOV and G. A. YUNITSKII, Zh. Fiz. Khim, 39 (1965) 2077.
6. R. W. GURNEY, Phys. Rev., 88 (1952) 465.
7. B. WUNDERLICH and H. BAUR, Adv. Poly. Sci., 7 (1970) 151.
8. J. A. KRUMHANSL and H. BROOKS, J. Chem. Phys., 21 (1953) 1663; J. C. BOWMAN and J. A. KRUMHANSL, J. Phys. Chem. Sol., 6 (1958) 367.
9. LANDOLT-BÖRNSTEIN, Physikalisch Chemische Tabellen, Springer-Verlag, Berlin, 1961, Ed. 6, Vol. 2, Part 4, p. 736; J. A. BEATTY, J. Math. Phys. (MIT), 6 (1926/27) 1.
10. B. WUNDERLICH, J. Chem. Phys., 37 (1962) 1207.
11. A widely spaced table is given by V. V. TARASOV, New Glass Physics Experiments, Gosstroizdat, Moscow, 1959.
12. H. WIEDEMEIER and F. J. CSILLAG, J. Crystal Growth, 46 (1979) 189.
13. H. WIEDEMEIER and G. PULTZ, to be published.
14. K. C. MILLS, Thermodynamic Data for Inorganic Sulfides, Selenides and Tellurides, Butterworths, London, 1974.
15. O. KUBACHEWSKI, E. L. EVANS and C. B. ALCOCK, Metallurgical Thermochemistry, Pergamon, Oxford, 1967.
16. V. M. ZHDANOV, Russ. J. Phys. Chem., 43 (1969) 1468.
17. H. WIEDEMEIER, P. SIEMERS, U. GAUR and B. WUNDERLICH, Thermochim. Acta, 27 (1978) 228.
18. V. M. ZHDANOV, Russ. J. Phys. Chem., 45 (1971) 1357.
19. D. H. PARKINSON and J. E. QUARRINGTON, Proc. Phys. Soc., 67 (1954) 569.
20. A. J. BEVOLO, H. R. SHANKS and D. E. ECKELS, Phys. Rev. B, 13 (1976) 3523.
21. H. WIEDEMEIER, G. PULTZ, U. GAUR and B. WUNDERLICH, Thermochim. Acta, in press.
22. W. W. WELLER and K. K. KELLEY, U. S. Bur. Mines Rept. Invest. (1964) 6511.
23. E. G. KING and S. S. TODD, J. Amer. Chem. Soc., 75 (1953) 3023.
24. V. V. TARASOV, V. M. ZHDANOV and A. K. MALTSEV, Russ. J. Phys. Chem., 42 (1968) 685.
25. W. NERNST and F. A. LINDEMANN, Z. Elecktrochem., 17 (1911) 817.
26. N. G. ALIEV, I. G. KERIMOV, M. M. KURBANOV and T. A. MANEDOV, Soviet Phys. Sol. State, 14 (1972) 1304.
27. Semiconducting II-VI, IV-VI and V-VI Compounds, Plenum, New York, 1969.
28. J. BURGEAT, G. LE ROUX and A. BRENAC, J. Appl. Cryst., 8 (1975) 325.
29. H. WIEDEMEIER and P. A. SIEMERS, Z. Anorg. Allgem. Chem., 411 (1975) 90.
30. H. WIEDEMEIER and P. A. SIEMERS, Z. Anorg. Allgem. Chem., 431 (1977) 299.
31. H. G. VON SCHNERING and H. WIEDEMEIER, Z. Krist., in press.
32. H. WIEDEMEIER and F. J. CSILLAG, Z. Krist., 149 (1979) 17.
33. H. WIEDEMEIER and H. G. VON SCHNERING, Z. Krist., 148 (1978) 295.
34. F. A. S. AL-ALAMY, A. A. BALCHIN and M. WHITE, J. Mat. Sci., 12 (1977) 2037.

35. W. NERNST, Ann. Physik, 36 (1911) 395.
36. K. KOMATSU and T. NAGAMIYA, J. Phys. Soc. Japan, 6 (1951) 438.
37. P. BLOEMBERGEN and A. R. MIEDEMA, Physica, 75 (1974) 205.
38. H. R. CHANDRASEKHAR, R. G. HUMPHREYS, U. ZWICK and M. CORDONA, Phys. Rev. B., 15 (1977) 2177.
39. P. M. NIKOLIC, L. MILJKOVIC, P. MIHAJLOVIC and B. LAURENCIC, J. Phys. C: Sol. St. Phys., 10 (1977) L289.
40. D. G. MEAD and J. C. IRWIN, Sol. State Commun., 20 (1976) 885.
41. H. R. CHANDRASEKHAR and U. ZWICK, Sol. State Commun., 18 (1976) 1509.
42. J. L. VEBLE and T. J. WIETLING, Sol. State Commun., 11 (1972) 941.
43. J. D. WILEY, W. J. BUKEL and R. L. SCHMIDT, Phys. Rev. B., 13 (1976) 2489.

**RÉSUMÉ** — On a examiné les capacités calorifiques à basses températures de 13 chalcogénure du groupe IV. Les capacités calorifiques des cristaux de structures principalement isotrope (GeTe, SnSe, SnTe, PbS, PbSe, PbTe) peuvent être représentées à  $\pm 3\%$ , par une fonction Debye à trois dimensions ( $\theta_3 = 205, 230, 175, 225, 150$  et 130 respectivement). Les capacités calorifiques des cristaux à structures anisotropes (GeS, GeSe, SnS, GeS<sub>2</sub>, GeSe<sub>2</sub> et SnS<sub>2</sub>) ne peuvent être représentées que par des paires de fonctions Debye à deux dimensions, pour les vibrations du réseau longitudinales et transversales (erreur de  $\pm 0,5$  à 3%;  $\theta_2(l) = 505, 345, 400, 705, 480$  et 570, et  $\theta_2(t) = 200, 185, 160, 175, 100$  et 265).

Comme il n'existe pas de tableaux détaillés pour la fonction Debye à deux dimensions les auteurs donnent en appendice un tableau à cinq positions. Des données Raman et infrarouges sont fournies à l'appui de cette analyse.

**ZUSAMMENFASSUNG** — Die Wärmekapazität bei niedrigen Temperaturen wurde für 13 Chalcogenide der Gruppe IV untersucht. Die Wärmekapazität der Kristalle von hauptsächlich isotroper Struktur (GeTe, SnSe, SnTe, PbS, PbSe, PbTe) kann innerhalb von  $\pm 3\%$  durch eine dreidimensionale Debye-Funktion dargestellt werden ( $\theta_3 = 205, 230, 175, 225, 150$  bzw. 130). Die Wärmekapazität von Kristallen anisotroper Struktur (GeS, GeSe, SnS, GeS<sub>2</sub>, GeSe<sub>2</sub> und SnS<sub>2</sub>) konnte für longitudinale und transversale Gittervibrationen nur durch Paare zweidimensionaler Debye-Funktionen dargestellt werden (Fehler:  $\pm 0,5$  bis 3%;  $\theta_2(l) = 505, 345, 400, 705, 480$  bzw. 570 und  $\theta_2(t) = 200, 185, 160, 175, 100$  bzw. 265).

Da die zweidimensionale Debye-Funktion nicht in allen Einzelheiten tabellarisiert worden ist, wird im Anhang eine fünfstellige Tafel dafür gegeben. Raman- und Infrarot-Angaben bestätigen diese Analyse.

**Резюме** — Исследованы низкотемпературные теплоемкости 13 халькогенидов группы IV. Теплоемкость кристаллов большой изотропной структуры (GeTe, SnSe, SnTe, PbS, PbSe, PbTe) может быть представлена с ошибкой  $\pm 3\%$  трехразмерной дебаевской функцией ( $\theta_3 = 205, 230, 175, 225, 150$  и 130, соответственно). Теплоемкость кристаллов с анизотропной структурой (GeS, GeSe, SnS, GeS<sub>2</sub>, GeSe<sub>2</sub>, и SnS<sub>2</sub>) может быть представлена только парой двухразмерных дебаевских функций для продольных и поперечных колебаний решетки (ошибка от  $\pm 0,5$  до 3%;  $\theta_2$  (прод.) = 505, 345, 400, 705, 480 и 570 для соответствующих соединений, а  $\theta_2$  (поп.) = 200, 185, 160, 175, 100 и 265). Поскольку двухразмерная дебаевская функция детально ранее не была приведена, авторы приводят ее в приложении. ИК спектры и спектры комбинационного рассеяния подтверждают проведенный анализ теплоемкостей.

### Appendix

The following table (Table 2) of  $C_v/3R$  as a function of  $\theta_2/T$  as given by the two-dimensional Debye function was calculated using Eq. 7 of the text. The computer program was based on "Simpson Rule" which states that by breaking the range of the definite integral ( $a \leq x \leq b$ ) into  $2n$  intervals of length  $h = (b - a)/2n$ , then approximately,

$$\int_a^b f(x)dx = \frac{h}{3} [f(x_0) + 4f(x_1) + 2f(x_2) + 4f(x_3) + \dots + 2f(x_{2n-2}) + 4f(x_{2n-1}) + f(x_{2n})]. \quad (1a)$$

The number of intervals was chosen to be 100, which leads to an error of less than  $+0.000001$  over the whole range of  $\theta_2/T$ . Above  $\theta_2/T = 17.50$  the two dimensional Debye function is represented to better than  $\pm 0.02\%$  by the low temperature approximation:

$$D_2(\theta/T) = 14.42468/(\theta/T)^2 \quad (2a)$$

Table 2  
Two-dimensional Debye function

Theta/T	Two-dimensional Debye function $C_V/3R$								
	0.00	0.01	0.02	0.03	0.04	0.05	0.06	0.07	0.08
0.00	1.00000	0.99999	0.99997	0.99995	0.99993	0.99989	0.99985	0.99979	0.99973
0.10	0.99958	0.99949	0.99939	0.99929	0.99918	0.99906	0.99893	0.99879	0.99864
0.20	0.99833	0.99816	0.99798	0.99779	0.99760	0.99739	0.99718	0.99696	0.99673
0.30	0.99625	0.99600	0.99574	0.99547	0.99519	0.99491	0.99462	0.99431	0.99400
0.40	0.99336	0.99303	0.99268	0.99234	0.99198	0.99161	0.99124	0.99086	0.99046
0.50	0.98966	0.98925	0.98883	0.98840	0.98796	0.98752	0.98706	0.98660	0.98613
0.60	0.98517	0.98468	0.98418	0.98367	0.98316	0.98263	0.98210	0.98157	0.98102
0.70	0.97991	0.97934	0.97876	0.97818	0.97759	0.97699	0.97638	0.97577	0.97515
0.80	0.97389	0.97324	0.97259	0.97194	0.97127	0.97060	0.96992	0.96924	0.96854
0.90	0.96713	0.96642	0.96570	0.96497	0.96424	0.96349	0.96274	0.96199	0.96122
1.00	0.95968	0.95889	0.95810	0.95731	0.95650	0.95569	0.95488	0.95405	0.95322
1.10	0.95154	0.95069	0.94984	0.94897	0.94810	0.94723	0.94635	0.94546	0.94456
1.20	0.94276	0.94184	0.94093	0.94000	0.93907	0.93813	0.93719	0.93624	0.93528
1.30	0.93336	0.93238	0.93140	0.93042	0.92943	0.92843	0.92743	0.92643	0.92541
1.40	0.92337	0.92234	0.92131	0.92027	0.91922	0.91817	0.91711	0.91605	0.91499
1.50	0.91283	0.91175	0.91067	0.90957	0.90847	0.90737	0.90626	0.90515	0.90404
1.60	0.90178	0.90065	0.89952	0.89838	0.89723	0.89608	0.89492	0.89376	0.89260
1.70	0.89026	0.88908	0.88790	0.88671	0.88552	0.88433	0.88313	0.88192	0.88072
1.80	0.87829	0.87707	0.87584	0.87462	0.87339	0.87215	0.87091	0.86967	0.86842
1.90	0.86592	0.86466	0.86340	0.86213	0.86086	0.85959	0.85831	0.85703	0.85575
2.00	0.85317	0.85188	0.85058	0.84929	0.84798	0.84668	0.84537	0.84406	0.84274
2.10	0.84010	0.83878	0.83745	0.83612	0.83479	0.83346	0.83212	0.83078	0.82944
2.20	0.82674	0.82539	0.82404	0.82268	0.82132	0.81996	0.81860	0.81723	0.81586
2.30	0.81312	0.81175	0.81037	0.80899	0.80761	0.80622	0.80484	0.80345	0.80206
2.40	0.79928	0.79788	0.79649	0.79509	0.79369	0.79229	0.79088	0.78948	0.78807
2.50	0.78525	0.78384	0.78243	0.78101	0.77960	0.77818	0.77676	0.77534	0.77392
2.60	0.77107	0.76965	0.76822	0.76679	0.76536	0.76393	0.76250	0.76107	0.75964
2.70	0.75677	0.75534	0.75390	0.75246	0.75103	0.74959	0.74815	0.74671	0.74383
2.80	0.74238	0.74094	0.73866	0.73661	0.73461	0.73228	0.73083	0.72939	0.72803

Two-dimensional Debye function

Theta/T	Two-dimensional Debye function C <sub>V</sub> /3R						
	0.00	0.01	0.02	0.03	0.04	0.05	0.06
2.90	0.72794	0.72649	0.72504	0.72360	0.72215	0.72070	0.71926
3.00	0.71346	0.71201	0.71057	0.70912	0.70767	0.70622	0.70478
3.10	0.69899	0.69754	0.69609	0.69465	0.69320	0.69176	0.69031
3.20	0.68454	0.68309	0.68165	0.68021	0.67877	0.67733	0.67589
3.30	0.67013	0.66870	0.66726	0.66582	0.66439	0.66296	0.66152
3.40	0.65580	0.65437	0.65294	0.65152	0.65009	0.64867	0.64725
3.50	0.64156	0.64014	0.63873	0.63731	0.63590	0.63448	0.63307
3.60	0.62743	0.62603	0.62462	0.62322	0.62182	0.62042	0.61902
3.70	0.61344	0.61205	0.61066	0.60927	0.60788	0.60650	0.60511
3.80	0.59959	0.59821	0.59684	0.59547	0.59410	0.59273	0.59136
3.90	0.58591	0.58455	0.58319	0.58183	0.58048	0.57913	0.57778
4.00	0.57240	0.57106	0.56972	0.56838	0.56705	0.56571	0.56438
4.10	0.55908	0.55776	0.55644	0.55512	0.55381	0.55250	0.55118
4.20	0.54596	0.54466	0.54336	0.54206	0.54077	0.53948	0.53819
4.30	0.53305	0.53177	0.53050	0.52922	0.52795	0.52668	0.52541
4.40	0.52036	0.51910	0.51785	0.51660	0.51535	0.51410	0.51286
4.50	0.50790	0.50666	0.50543	0.50420	0.50298	0.50175	0.50053
4.60	0.49566	0.49445	0.49325	0.49204	0.49084	0.48964	0.48844
4.70	0.48367	0.48248	0.48130	0.48012	0.47894	0.47776	0.47659
4.80	0.47192	0.47075	0.46960	0.46844	0.46728	0.46613	0.46498
4.90	0.46041	0.45927	0.45814	0.45700	0.45587	0.45475	0.45362
5.00	0.44915	0.44804	0.44692	0.44582	0.44471	0.44361	0.44251
5.10	0.43814	0.43705	0.43596	0.43488	0.43380	0.43273	0.43165
5.20	0.42737	0.42631	0.42525	0.42420	0.42314	0.42209	0.42104
5.30	0.41686	0.41583	0.41479	0.41376	0.41273	0.41170	0.41068
5.40	0.40660	0.40559	0.40458	0.40357	0.40257	0.40156	0.40056
5.50	0.39659	0.39560	0.39462	0.39363	0.39265	0.39168	0.39070
5.60	0.38682	0.38586	0.38490	0.38394	0.38299	0.38203	0.38108
5.70	0.37730	0.37636	0.37543	0.37449	0.37356	0.37263	0.37171

5.80	0.36802	0.36711	0.35899	0.35810	0.35721	0.35632	0.35544	0.35516	0.35368	0.35193	0.35106
5.90			0.35019	0.34932	0.34845	0.34759	0.34673	0.34587	0.34502	0.34417	0.34331
6.00			0.34162	0.34077	0.33993	0.33909	0.33826	0.33742	0.33659	0.33576	0.33493
6.10			0.33328	0.33246	0.33164	0.33082	0.33001	0.32920	0.32839	0.32759	0.32677
6.20			0.32517	0.32437	0.32357	0.32278	0.32199	0.32120	0.32041	0.31962	0.31884
6.30			0.31650	0.31573	0.31495	0.31418	0.31341	0.31265	0.31188	0.31112	0.31036
6.40			0.30961	0.30885	0.30810	0.30735	0.30660	0.30585	0.30510	0.30436	0.30362
6.50			0.30215	0.30141	0.30068	0.29995	0.29922	0.29849	0.29777	0.29705	0.29633
6.60			6.70	0.29489	0.29418	0.29347	0.29276	0.29205	0.29134	0.28964	0.28894
			6.80	0.28784	0.28715	0.28646	0.28577	0.28508	0.28440	0.28371	0.28303
			6.90	0.28100	0.28032	0.27965	0.27898	0.27831	0.27764	0.27698	0.27632
			7.00	0.27434	0.27369	0.27303	0.27238	0.27173	0.27108	0.27044	0.26980
			7.10	0.26788	0.26724	0.26660	0.26597	0.26534	0.26471	0.26409	0.26346
			7.20	0.26159	0.26098	0.26036	0.25975	0.25913	0.25852	0.25791	0.25670
			7.30	0.25549	0.25489	0.25429	0.25370	0.25310	0.25251	0.25192	0.25074
			7.40	0.24957	0.24899	0.24840	0.24782	0.24725	0.24667	0.24610	0.24495
			7.50	0.24381	0.24325	0.24268	0.24212	0.24156	0.24100	0.24044	0.23989
			7.60	0.23823	0.23767	0.23713	0.23658	0.23603	0.23549	0.23495	0.23441
			7.70	0.23280	0.23226	0.23173	0.23120	0.23067	0.23014	0.22962	0.22909
			7.80	0.22753	0.22701	0.22649	0.22597	0.22546	0.22495	0.22444	0.22393
			7.90	0.22241	0.22190	0.22140	0.22090	0.22040	0.21990	0.21941	0.21891
			8.00	0.21744	0.21695	0.21646	0.21597	0.21549	0.21501	0.21452	0.21404
			8.10	0.21261	0.21213	0.21166	0.21119	0.21072	0.21025	0.20978	0.20931
			8.20	0.20792	0.20746	0.20700	0.20654	0.20608	0.20563	0.20517	0.20472
			8.30	0.20337	0.20292	0.20247	0.20203	0.20158	0.20114	0.20070	0.20026
			8.40	0.19894	0.19851	0.19807	0.19764	0.19721	0.19678	0.19635	0.19592
			8.50	0.19465	0.19422	0.19380	0.19338	0.19296	0.19255	0.19213	0.19171
			8.60	0.19047	0.19006	0.18965	0.18925	0.18884	0.18843	0.18803	0.18762
			8.70	0.18642	0.18602	0.18562	0.18523	0.18483	0.18444	0.18404	0.18365
			8.80	0.18248	0.18209	0.18171	0.18132	0.18094	0.18056	0.18017	0.17979
			8.90	0.17866	0.17828	0.17790	0.17753	0.17716	0.17678	0.17641	0.17604
			9.00	0.17494	0.17457	0.17421	0.17384	0.17348	0.17312	0.17276	0.17240
			9.10	0.17132	0.17061	0.17097	0.17061	0.16991	0.16956	0.16886	0.16816

Two-dimensional Debye function

Theta/T	Two-dimensional Debye function C <sub>V</sub> /3R						
	0.00	0.01	0.02	0.03	0.04	0.05	0.06
9.20	0.16781	0.16747	0.16712	0.16678	0.16644	0.16609	0.16575
9.30	0.16440	0.16406	0.16373	0.16339	0.16306	0.16273	0.16240
9.40	0.16108	0.16075	0.16043	0.16010	0.15978	0.15946	0.15913
9.50	0.15785	0.15754	0.15722	0.15690	0.15659	0.15627	0.15596
9.60	0.15472	0.15441	0.15410	0.15379	0.15349	0.15318	0.15288
9.70	0.15167	0.15137	0.15107	0.15077	0.15047	0.15017	0.14988
9.80	0.14870	0.14841	0.14812	0.14783	0.14754	0.14725	0.14696
9.90	0.14581	0.14553	0.14525	0.14496	0.14468	0.14440	0.14412
10.00	0.14301	0.14273	0.14245	0.14218	0.14190	0.14163	0.14136
10.10	0.14027	0.14001	0.13974	0.13947	0.13920	0.13894	0.13867
10.20	0.13762	0.13735	0.13709	0.13683	0.13657	0.13631	0.13606
10.30	0.13503	0.13477	0.13452	0.13427	0.13401	0.13376	0.13351
10.40	0.13251	0.13226	0.13201	0.13177	0.13152	0.13127	0.13103
10.50	0.13006	0.12982	0.12958	0.12933	0.12910	0.12886	0.12862
10.60	0.12767	0.12743	0.12720	0.12697	0.12673	0.12650	0.12627
10.70	0.12534	0.12512	0.12489	0.12466	0.12443	0.12421	0.12398
10.80	0.12308	0.12286	0.12263	0.12241	0.12219	0.12197	0.12175
10.90	0.12087	0.12066	0.12044	0.12022	0.12001	0.11979	0.11958
11.00	0.11872	0.11851	0.11830	0.11809	0.11788	0.11767	0.11746
11.10	0.11663	0.11642	0.11622	0.11601	0.11581	0.11560	0.11540
11.20	0.11459	0.11439	0.11419	0.11399	0.11379	0.11359	0.11339
11.30	0.11260	0.11240	0.11221	0.11201	0.11182	0.11162	0.11143
11.40	0.11066	0.11047	0.11028	0.11009	0.10990	0.10971	0.10952
11.50	0.10877	0.10858	0.10839	0.10821	0.10802	0.10784	0.10765
11.60	0.10692	0.10674	0.10656	0.10638	0.10620	0.10602	0.10584
11.70	0.10512	0.10494	0.10477	0.10459	0.10441	0.10424	0.10406
11.80	0.10337	0.10319	0.10302	0.10285	0.10267	0.10250	0.10233
11.90	0.10165	0.10148	0.10131	0.10115	0.10098	0.10081	0.10061
12.00	0.09998	0.09982	0.09965	0.09949	0.09932	0.09916	0.09883

12.10	0.09835	0.09819	0.09803	0.09787	0.09771	0.09755	0.09739	0.09723	0.09707
12.20	0.09676	0.09660	0.09644	0.09628	0.09613	0.09597	0.09582	0.09566	0.09551
12.30	0.09520	0.09505	0.09489	0.09474	0.09459	0.09444	0.09428	0.09413	0.09398
12.40	0.09368	0.09353	0.09338	0.09323	0.09308	0.09294	0.09279	0.09264	0.09249
12.50	0.09220	0.09205	0.09191	0.09176	0.09161	0.09147	0.09132	0.09118	0.09104
12.60	0.09075	0.09061	0.09046	0.09032	0.09019	0.09004	0.08990	0.08976	0.08961
12.70	0.08933	0.08919	0.08905	0.08892	0.08878	0.08864	0.08850	0.08836	0.08823
12.80	0.08795	0.08781	0.08768	0.08754	0.08741	0.08727	0.08714	0.08700	0.08687
12.90	0.08660	0.08647	0.08633	0.08620	0.08607	0.08594	0.08580	0.08567	0.08551
13.00	0.08528	0.08515	0.08502	0.08489	0.08476	0.08463	0.08450	0.08437	0.08424
13.10	0.08399	0.08386	0.08373	0.08361	0.08348	0.08335	0.08323	0.08310	0.08297
13.20	0.08272	0.08260	0.08248	0.08235	0.08223	0.08210	0.08198	0.08186	0.08173
13.30	0.08149	0.08137	0.08125	0.08112	0.08100	0.08088	0.08076	0.08064	0.08052
13.40	0.08028	0.08016	0.08004	0.07993	0.07981	0.07969	0.07957	0.07945	0.07934
13.50	0.07910	0.07898	0.07887	0.07875	0.07864	0.07852	0.07840	0.07829	0.07817
13.60	0.07795	0.07783	0.07772	0.07760	0.07749	0.07738	0.07726	0.07715	0.07704
13.70	0.07681	0.07670	0.07659	0.07648	0.07637	0.07627	0.07615	0.07604	0.07593
13.80	0.07571	0.07560	0.07549	0.07538	0.07527	0.07516	0.07506	0.07495	0.07484
13.90	0.07463	0.07452	0.07441	0.07431	0.07420	0.07409	0.07399	0.07388	0.07378
14.00	0.07357	0.07346	0.07336	0.07325	0.07315	0.07304	0.07294	0.07284	0.07273
14.10	0.07263	0.07243	0.07232	0.07222	0.07212	0.07202	0.07192	0.07182	0.07171
14.20	0.07151	0.07141	0.07131	0.07121	0.07111	0.07101	0.07091	0.07081	0.07072
14.30	0.07052	0.07042	0.07032	0.07022	0.07013	0.07003	0.06993	0.06983	0.06974
14.40	0.06954	0.06945	0.06935	0.06925	0.06916	0.06906	0.06897	0.06887	0.06878
14.50	0.06859	0.06849	0.06840	0.06831	0.06821	0.06812	0.06803	0.06793	0.06784
14.60	0.06765	0.06756	0.06747	0.06738	0.06729	0.06719	0.06710	0.06701	0.06692
14.70	0.06674	0.06665	0.06656	0.06647	0.06638	0.06629	0.06620	0.06611	0.06602
14.80	0.06584	0.06575	0.06566	0.06557	0.06549	0.06540	0.06531	0.06522	0.06514
14.90	0.06496	0.06487	0.06479	0.06470	0.06461	0.06453	0.06444	0.06436	0.06427
15.00	0.06410	0.06401	0.06393	0.06384	0.06376	0.06367	0.06359	0.06350	0.06342
15.10	0.06325	0.06317	0.06309	0.06300	0.06292	0.06284	0.06275	0.06267	0.06259
15.20	0.06242	0.06234	0.06226	0.06218	0.06210	0.06202	0.06193	0.06185	0.06177
15.30	0.06161	0.06153	0.06145	0.06137	0.06129	0.06121	0.06113	0.06105	0.06097
15.40	0.06081	0.06066	0.06058	0.06050	0.06042	0.06034	0.06027	0.06019	0.06011

Two-dimensional Debye function

Theta/T	Two-dimensional Debye function $C_v/3R$							
	0.00	0.01	0.02	0.03	0.04	0.05	0.06	0.07
15.50	0.06003	0.05996	0.05988	0.05980	0.05972	0.05965	0.05957	0.05949
15.60	0.05927	0.05919	0.05911	0.05904	0.05896	0.05889	0.05881	0.05874
15.70	0.05851	0.05844	0.05837	0.05829	0.05822	0.05814	0.05807	0.05800
15.80	0.05778	0.05770	0.05763	0.05756	0.05749	0.05741	0.05734	0.05727
15.90	0.05705	0.05698	0.05691	0.05684	0.05677	0.05670	0.05663	0.05655
16.00	0.05634	0.05627	0.05620	0.05613	0.05606	0.05599	0.05592	0.05585
16.10	0.05564	0.05558	0.05551	0.05544	0.05537	0.05530	0.05523	0.05516
16.20	0.05496	0.05489	0.05482	0.05476	0.05469	0.05462	0.05456	0.05449
16.30	0.05429	0.05422	0.05416	0.05409	0.05402	0.05396	0.05389	0.05376
16.40	0.05363	0.05356	0.05350	0.05343	0.05337	0.05330	0.05324	0.05317
16.50	0.05298	0.05292	0.05285	0.05279	0.05272	0.05266	0.05260	0.05253
16.60	0.05234	0.05228	0.05222	0.05216	0.05209	0.05203	0.05197	0.05191
16.70	0.05172	0.05166	0.05160	0.05153	0.05147	0.05141	0.05135	0.05129
16.80	0.05111	0.05104	0.05098	0.05092	0.05086	0.05080	0.05074	0.05068
16.90	0.05050	0.05044	0.05038	0.05032	0.05026	0.05021	0.05015	0.05009
17.00	0.04991	0.04985	0.04979	0.04973	0.04968	0.04962	0.04956	0.04950
17.10	0.04933	0.04927	0.04921	0.04916	0.04910	0.04904	0.04898	0.04893
17.20	0.04876	0.04870	0.04864	0.04859	0.04853	0.04847	0.04842	0.04836
17.30	0.04819	0.04814	0.04808	0.04803	0.04797	0.04792	0.04786	0.04781
17.40	0.04764	0.04759	0.04753	0.04748	0.04742	0.04737	0.04732	0.04726